VERITAS Dark Matter search in Dwarf Spheroidal galaxies

On behalf of VERITAS Collaboration **Chiara Giuri (DESY, Zeuthen)**

MAGIC Dark Matter Workshop

Barcelona, 17.01.19

HELMHOLTZ RESEARCH FOR GRAND CHALLENGES

HELMHOLTZ Young Investigators

VERITAS

Universität Potsdam

DESY.

Introduction to VERITAS

- Located at the Fred Lawrence Whipple Observatory (FLWO) in southern Arizona (31 40N, 110 57W, 1.3km a.s.l.)
- Array of four 12 m telescopes separated ~100 m each other
- Energy range: **85 GeV to 30 TeV**
- **FoV ~ 3.5°**, each camera has 499 PMTs
- Fully operational since 2007 (V4), then **two major upgrades**:
  - ➡ In 2009 T1 was relocated (V5)
  - ➡ In 2012 new higher quantum efficiency PMTs (V6)
- Every year ~ **1000 hrs** dark **+ 200 hrs** under bright moonlight conditions (since 2012)

VERITAS Dark Matter Targets

Dwarf Galaxies:
- High mass to light ratio
- Close by (~10's kpc)
- No known astrophysical background

Galactic center:
- High DM content
- Close by (~8 kpc)
- High astrophysical background

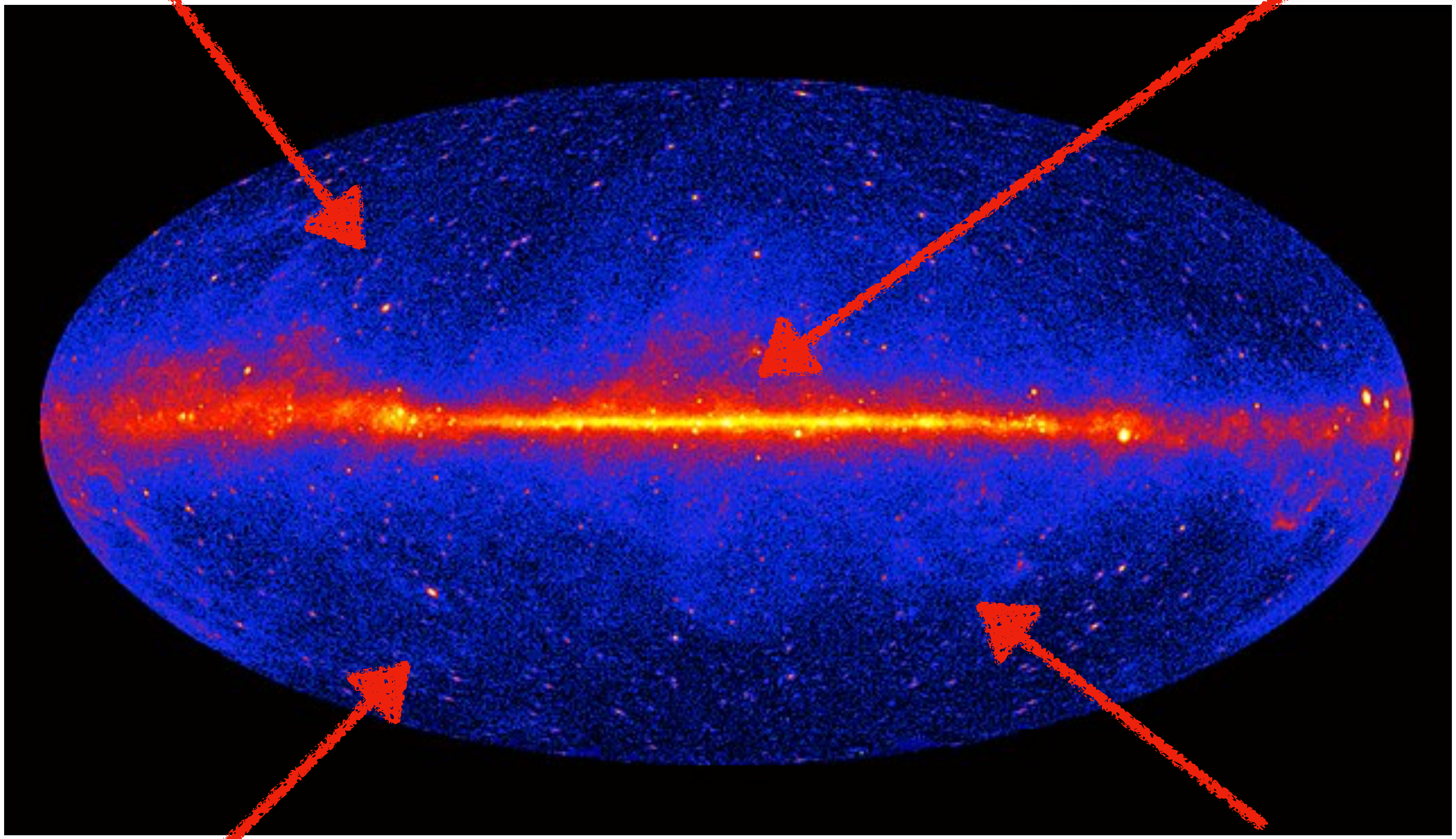

***Fermi* Unidentified Objects:**
- DM subhalos?
- Two suitable candidates in the 2FGL observed by VERITAS

Galaxy clusters:
- Large DM content (~80% of their masses)
- Very distant (~10's Mpc)

Why searching for Dark Matter in dSphs?

Extremely large mass to light ratio

Nearby systems to look for DM (tens to hundreds kpc away)

Most DM dominated stellar systems known in the Universe

Free from other sources of gamma-ray emission

High Galactic latitudes (barely affected by diffuse astrophysical foregrounds from Milky Way)

Formed early, probe galaxy formation and evolution

VERITAS dSphs observations: 2007-2017

J-factors from Geringer-Sameth et al., 2015 (J_1) and Bonnivard et al., 2015 (J_2)

Dwarf	$\log_{10} J_1(0.5°)$ [GeV^2 cm^{-5}]	$\log_{10} J_2(0.5°)$ [GeV^2 cm^{-5}]	$\log_{10} D_1(0.5°)$ [GeV cm^{-2}]	Exposure v4 [min]	Exposure v5 [min]	Exposure v6 [min]	Total Exposure [min]
Segue 1	$19.4^{+0.3}_{-0.4}$	$17.0^{+2.1}_{-2.2}$	$18.0^{+0.2}_{-0.3}$	0	6121	4921	11042
Ursa Major II	$19.4^{+0.4}_{-0.4}$	$19.9^{+0.7}_{-0.5}$	$18.4^{+0.3}_{-0.3}$	0	0	10869	10869
Ursa Minor	$18.9^{+0.3}_{-0.2}$	$19.0^{+0.1}_{-0.1}$	$18.0^{+0.2}_{-0.1}$	711	2209	6844	9724
Draco	$18.8^{+0.1}_{-0.1}$	$19.1^{+0.4}_{-0.2}$	$18.5^{+0.1}_{-0.1}$	1169	2170	3435	6813
Coma Berencies	$19.0^{+0.4}_{-0.4}$	$19.6^{+0.8}_{-0.7}$	$18.0^{+0.2}_{-0.3}$	0	0	2204	2204
Segue II	$16.2^{+1.1}_{-1.0}$	$18.9^{+1.1}_{-1.1}$	$15.9^{+0.4}_{-0.4}$	0	0	1128	1128
Boötes 1	$18.2^{+0.4}_{-0.4}$	$18.5^{+0.6}_{-0.4}$	$17.9^{+0.2}_{-0.3}$	960	0	0	960
Leo II	$18.0^{+0.2}_{-0.2}$	$17.8^{+0.2}_{-0.2}$	$17.2^{+0.4}_{-0.5}$	0	0	946	946
Willman 1	N/A	N/A	N/A	931	0	0	931
Triangulum II	N/A	N/A	N/A	0	0	909	909
Canes Ver. II	$17.7^{+0.5}_{-0.4}$	$18.5^{+1.2}_{-0.9}$	$17.0^{+0.2}_{-0.2}$	0	0	864	864
Canes Ver. I	$17.4^{+0.4}_{-0.3}$	$17.5^{+0.4}_{-0.2}$	$17.6^{+0.4}_{-0.7}$	0	0	850	850
Hercules I	$16.9^{+0.7}_{-0.7}$	$17.5^{+0.7}_{-0.7}$	$16.7^{+0.4}_{-0.4}$	0	0	794	794
Sextans I	$18.0^{+0.2}_{-0.2}$	$17.6^{+0.2}_{-0.2}$	$17.9^{+0.1}_{-0.2}$	0	0	783	783
Draco II	N/A	N/A	N/A	0	0	598	598
Ursa Major I	$17.9^{+0.6}_{-0.3}$	$18.7^{+0.6}_{-0.5}$	$17.6^{+0.2}_{-0.4}$	0	0	482	482
Leo I	$17.8^{+0.2}_{-0.2}$	$17.8^{+0.5}_{-0.2}$	$17.9^{+0.2}_{-0.2}$	0	0	409	409
Leo V	$16.4^{+0.9}_{-0.9}$	$16.1^{+1.2}_{-1.0}$	$15.9^{+0.5}_{-0.5}$	0	0	167	167
Leo IV	$16.3^{+1.1}_{-1.7}$	$16.2^{+1.5}_{-1.6}$	$16.1^{+0.7}_{-1.1}$	0	0	151	151

"Survey" dSphs: covering nearly all Northern Hemisphere dSphs

"Deep Exposure" dSphs: with the best J-factor in literature

VERITAS dSphs observations: 2007-2017

J-factors from Geringer-Sameth et al., 2015 (J_1) and Bonnivard et al., 2015 (J_2)

Dwarf	$\log_{10} J_1(0.5^\circ)$ [GeV^2 cm^{-5}]	$\log_{10} J_2(0.5^\circ)$ [GeV^2 cm^{-5}]	$\log_{10} D_1(0.5^\circ)$ [GeV cm^{-2}]	Exposure v4 [min]	Exposure v5 [min]	Exposure v6 [min]	Total Exposure [min]
Segue 1	$19.4^{+0.3}_{-0.4}$	$17.0^{+2.1}_{-2.2}$	$18.0^{+0.2}_{-0.3}$	0	6121	4921	11042
Ursa Major II	$19.4^{+0.4}_{-0.4}$	$19.9^{+0.7}_{-0.5}$	$18.4^{+0.3}_{-0.3}$	0	0	10869	10869
Ursa Minor	$18.9^{+0.3}_{-0.2}$	$19.0^{+0.1}_{-0.1}$	$18.0^{+0.2}_{-0.1}$	711	2209	6844	9724
Draco	$18.8^{+0.1}_{-0.1}$	$19.1^{+0.4}_{-0.2}$	$18.5^{+0.1}_{-0.1}$	1169	2170	3435	6813
Coma Berencies	$19.0^{+0.4}_{-0.4}$	$19.6^{+0.8}_{-0.7}$	$18.0^{+0.2}_{-0.3}$	0	0	2204	2204

Majority of
Dwarf time allocation

Classical dSphs $(L > 10^5 L_{sol})$ and
ultra-faint dSphs $(L = 10^{3-5} L_{sol})$

1. Time is divided among different sources
2. Mitigates **against wrong** estimation of J profile (e.g., Segue 1)

"Deep Exposure" dSphs: with the best J-factor in literature

VERITAS dSphs observations: 2007-2017

J-factors from Geringer-Sameth et al., 2015 (J_1) and Bonnivard et al., 2015 (J_2)

Shorter observing times

Dwarf	$\log_{10} J_1(0.5°)$ [GeV^2 cm^{-5}]	$\log_{10} J_2(0.5°)$ [GeV^2 cm^{-5}]	$\log_{10} D_1(0.5°)$ [GeV cm^{-2}]	Exposure v4 [min]	Exposure v5 [min]	Exposure v6 [min]	Total Exposure [min]
Segue II	$16.2^{+1.1}_{-1.0}$	$18.9^{+1.1}_{-1.1}$	$15.9^{+0.4}_{-0.4}$	0	0	1128	1128
Boötes 1	$18.2^{+0.4}_{-0.4}$	$18.5^{+0.6}_{-0.4}$	$17.9^{+0.2}_{-0.3}$	960	0	0	960
Leo II	$18.0^{+0.2}_{-0.2}$	$17.8^{+0.2}_{-0.2}$	$17.2^{+0.4}_{-0.5}$	0	0	946	946
Willman 1	N/A	N/A	N/A	931	0	0	931
Triangulum II	N/A	N/A	N/A	0	0	909	909
Canes Ver. II	$17.7^{+0.5}_{-0.4}$	$18.5^{+1.2}_{-0.9}$	$17.0^{+0.2}_{-0.2}$	0	0	864	864
Canes Ver. I	$17.4^{+0.4}_{-0.3}$	$17.5^{+0.4}_{-0.2}$	$17.6^{+0.4}_{-0.7}$	0	0	850	850
Hercules I	$16.9^{+0.7}_{-0.7}$	$17.5^{+0.7}_{-0.7}$	$16.7^{+0.4}_{-0.4}$	0	0	794	794
Sextans I	$18.0^{+0.2}_{-0.2}$	$17.6^{+0.2}_{-0.2}$	$17.9^{+0.1}_{-0.2}$	0	0	783	783
Draco II	N/A	N/A	N/A	0	0	598	598
Ursa Major I	$17.9^{+0.6}_{-0.3}$	$18.7^{+0.6}_{-0.5}$	$17.6^{+0.2}_{-0.4}$	0	0	482	482
Leo I	$17.8^{+0.2}_{-0.2}$	$17.8^{+0.5}_{-0.2}$	$17.9^{+0.2}_{-0.2}$	0	0	409	409
Leo V	$16.4^{+0.9}_{-0.9}$	$16.1^{+1.2}_{-1.0}$	$15.9^{+0.5}_{-0.5}$	0	0	167	167
Leo IV	$16.3^{+1.1}_{-1.7}$	$16.2^{+1.5}_{-1.6}$	$16.1^{+0.7}_{-1.1}$	0	0	151	151

"Survey" dSphs: covering nearly all Northern Hemisphere dSphs

Combined analysis of dSphs from 2007 to 2013

216 hrs of VERITAS data

J-factors from Geringer-Sameth et al., 2015

DSph	N_{ON} [counts]	N_{OFF} [counts]	$\bar{\alpha}$	Significance [σ]	$N^{95\%}$ [counts]	$\Phi^{95\%}$ [10^{-12}cm^{2}s^{-1}]	Distance [kpc]	$\log_{10} J(0.17°)$ [GeV^2 cm^{-5}]
Segue 1	15895	120826	0.131	0.7	235.8	0.34	23	$19.2^{+0.3}_{-0.3}$
Draco	4297	39472	0.111	-1.0	33.5	0.15	76	$18.3^{+0.1}_{-0.1}$
Ursa Minor	4181	35790	0.119	-0.1	91.6	0.37	76	$18.9^{+0.3}_{-0.3}$
Boötes 1	1206	10836	0.116	-1.0	34.5	0.40	66	$18.3^{+0.3}_{-0.4}$
Willman 1	1926	18187	0.108	-0.6	23.5	0.39	38	N/A

Not calculated due to irregular kinematics

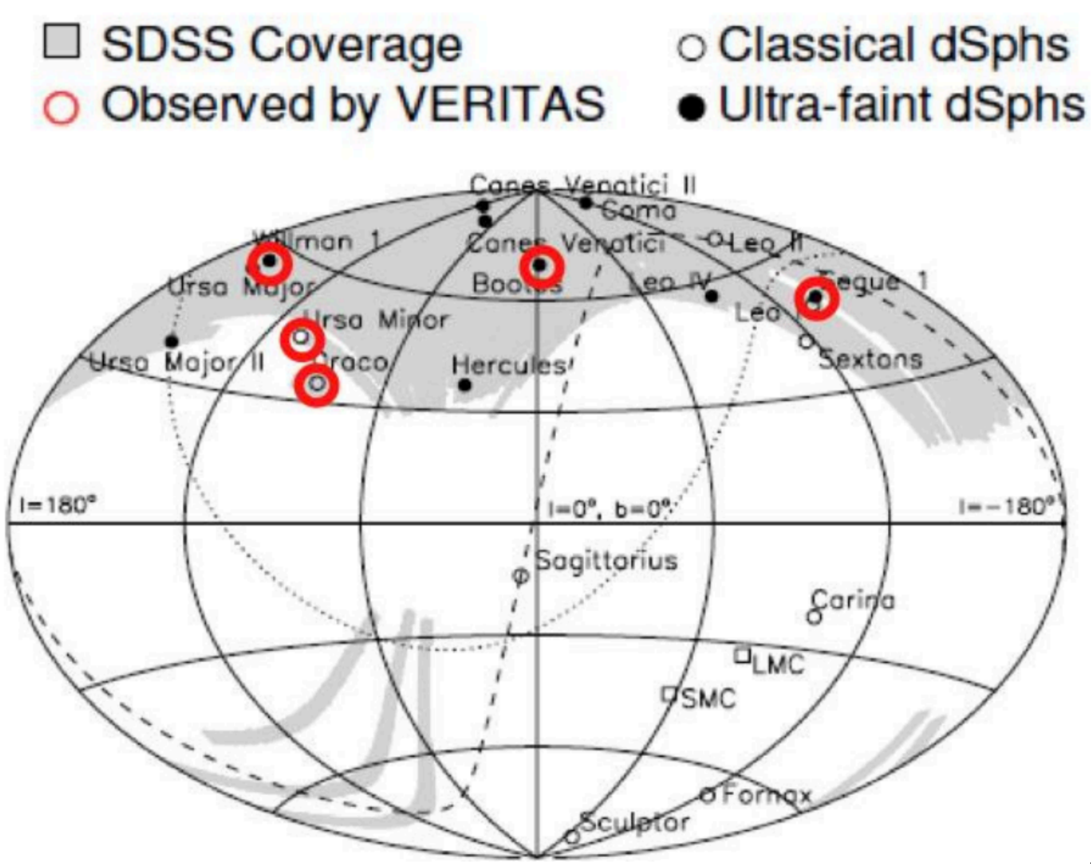

No gamma-ray detection

Combined analysis of dSphs from 2007 to 2013

J factors from Geringer-Sameth et al., 2015

- Consider spherically symmetric density profile

$$\rho(r) = \frac{\rho_s}{(r/r_s)^\gamma \left[1 + (r/r_s)^\alpha\right]^{(\beta-\gamma)/\alpha}},$$

(Zhao et al 1996)

- Annihilation flux depends on source's gravitational potential
- Assumptions:
  1. Dynamic equilibrium and spherical symmetry
  2. Stars distributed according to Plummer profile
  3. The distribution of stellar velocities is not influenced by presence of binary stars
  4. Stars negligibly affect gravitational potential

$$\frac{1}{\nu(r)}\frac{d}{dr}[\nu(r)\overline{u_r^2}(r)] + 2\frac{\beta_a(r)\overline{u_r^2}(r)}{r} = -\frac{d\Phi}{dr} = -\frac{GM(r)}{r^2}$$

Mass profile relates to observable profiles

$$\sigma^2(R)\Sigma(R) = 2\int_R^\infty \left(1 - \beta_a(r)\frac{R^2}{r^2}\right)\frac{\nu(r)\,\overline{u_r^2}(r)\,r}{\sqrt{r^2 - R^2}}\,dr.$$

Used to fit models for ρ(r) to observed velocity dispersion and surface brightness profiles

Combined analysis of dSphs from 2007 to 2013

J factors from Geringer-Sameth et al., 2015

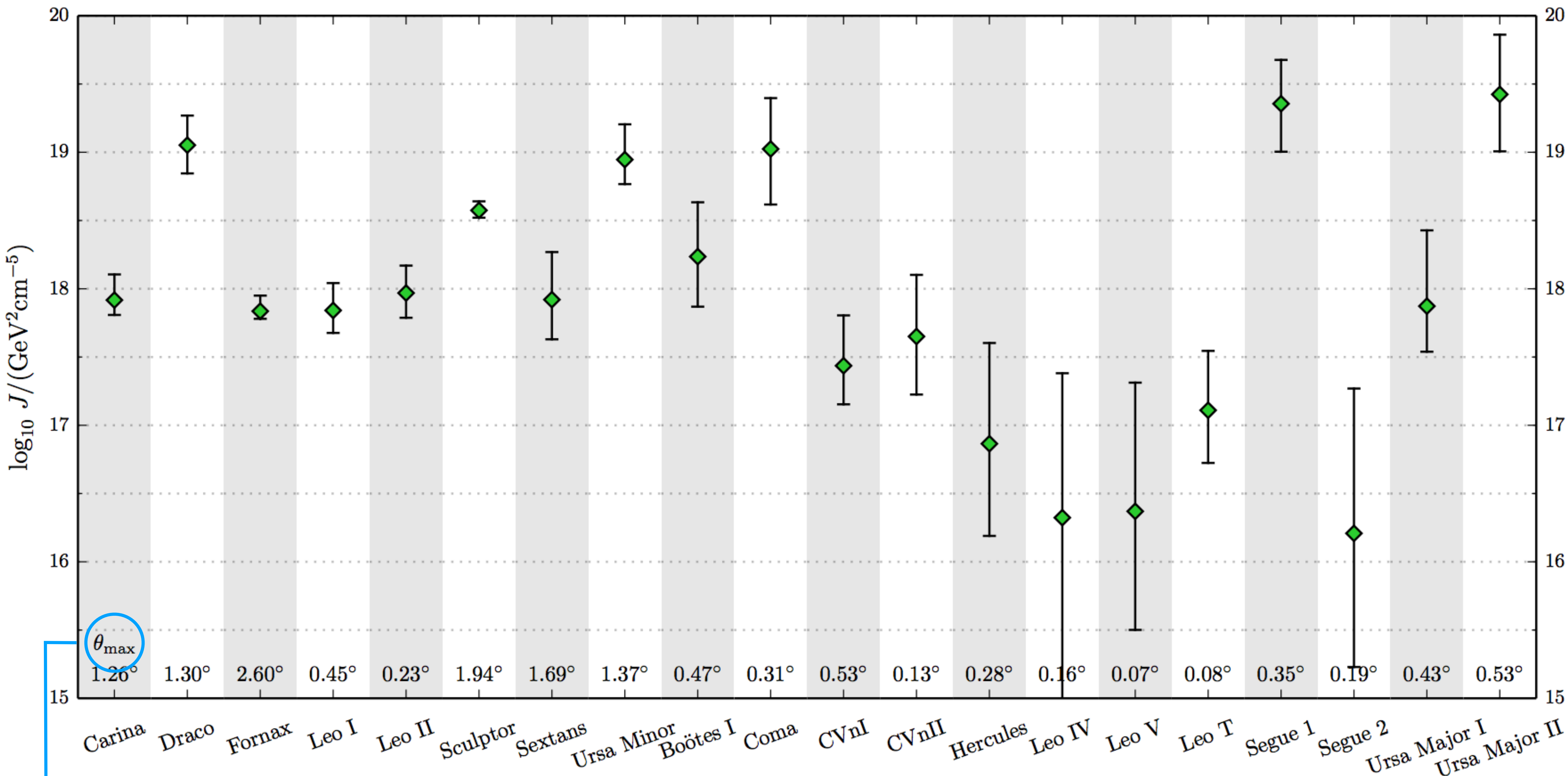

$= arcsin(r_{max}/D)$ where r_{max} distance from dwarf center to outermost star

Combined analysis of dSphs from 2007 to 2013

"Crescent" background method used in combined dSphs analysis

For the first time applied to IACTs

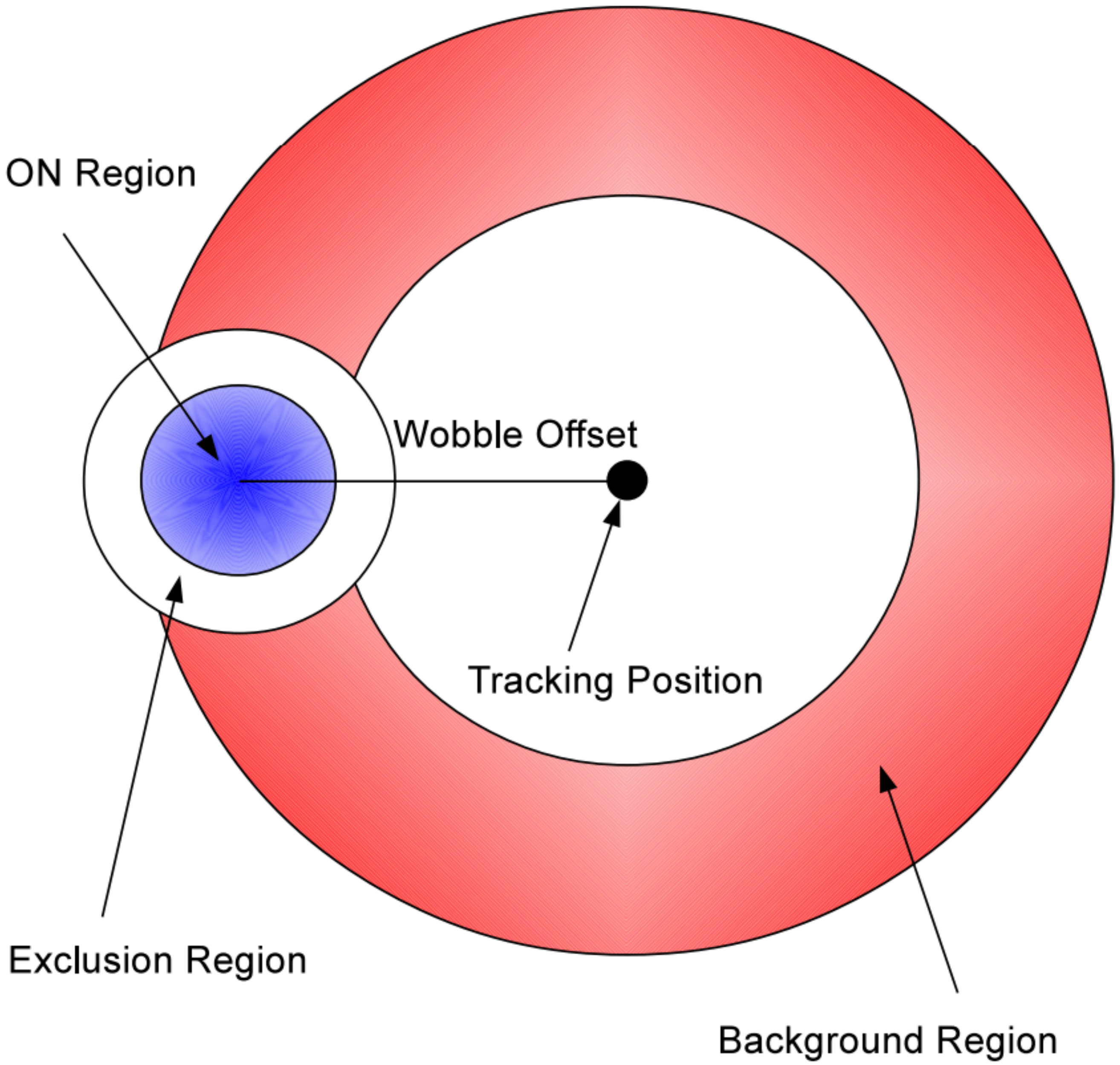

Background events selected from an annulus

Annulus centered on tracking position

Factor two more background events than reflected regions

Reduced energy dependence of the background scaling factor

Combined analysis of dSphs from 2007 to 2013

Event Weighting method A. Geringer-Sameth, S. M. Koushiappas, and M. G. Walker, Phys. Rev. D 91, 083535 (2015).

→ For the first time applied to IACTs

- In ON region, each event has a weight based on:
  1. Dwarf field ν it came from → For the first time
  2. Reconstructed energy E
  3. Reconstructed angular separation from the dwarf θ

"Optimal" test → Maximization of statistical power of hypothesis test

Test statistic **T** → $T = \sum_i w_i$ → $w = \log\left[1 + \frac{s}{b}\right]$

Combined analysis of dSphs from 2007 to 2013

Event Weighting method

A. Geringer-Sameth, S. M. Koushiappas, and M. G. Walker, Phys. Rev. D 91, 083535 (2015).

Where..

Expected number of signal events

$$s(\nu, E, \theta) = \frac{dN(\nu, E, \theta)}{dE d\Omega} dE 2\pi \sin(\theta) d\theta$$

Given by convolving gamma-ray flux from annihilation with the VERITAS response function

$$\frac{dN(E,\hat{\mathbf{n}})}{dE d\Omega} = \int_{E_t} \int_{\Omega_t} dE_t d\Omega_t \frac{dF(E_t,\hat{\mathbf{n}}_t)}{dE_t d\Omega_t} R(E,\hat{\mathbf{n}}|E_t,\hat{\mathbf{n}}_t)$$

$$\frac{dF(E,\hat{\mathbf{n}})}{dE d\Omega} = \frac{\langle\sigma v\rangle}{8\pi M^2} \frac{dN_\gamma(E)}{dE} \frac{dJ(\hat{\mathbf{n}})}{d\Omega}$$

$$R(E,\hat{\mathbf{n}}|E_t,\hat{\mathbf{n}}_t) = \sum_{\text{runs}} \tau A_{\text{eff}}(E_t) \text{PSF}(\hat{\mathbf{n}}|E_t,\hat{\mathbf{n}}_t) D(E|E_t)$$

Combined analysis of dSphs from 2007 to 2013

Event Weighting method

A. Geringer-Sameth, S. M. Koushiappas, and M. G. Walker, Phys. Rev. D 91, 083535 (2015).

Where..

$$\frac{dN_\gamma(E)}{dE} = \sum_i B_i \frac{dN_{\gamma,i}(E)}{dE}$$

→ Spectrum of gamma-ray for a single annihilation event

PSF → Derived from gamma-ray simulations → Larger statistics

A_{eff} → Depends on true gamma-ray energy, zenith and azimuth angles, background noise, configuration epoch, offset, cuts

$D(E|E_t)$ → Energy dispersion: quantifies energy resolution and bias of VERITAS

Combined analysis of dSphs from 2007 to 2013

Systematic uncertainties

1. Imperfect knowledge of DM density profile: different DM halos fit the kinematic observables

2. Wrong calculation of velocity dispersion leads to mis-estimate of J profiles (e.g., **Segue 1 excluded**)

→ Shaded bands 1σ systematic uncertainty

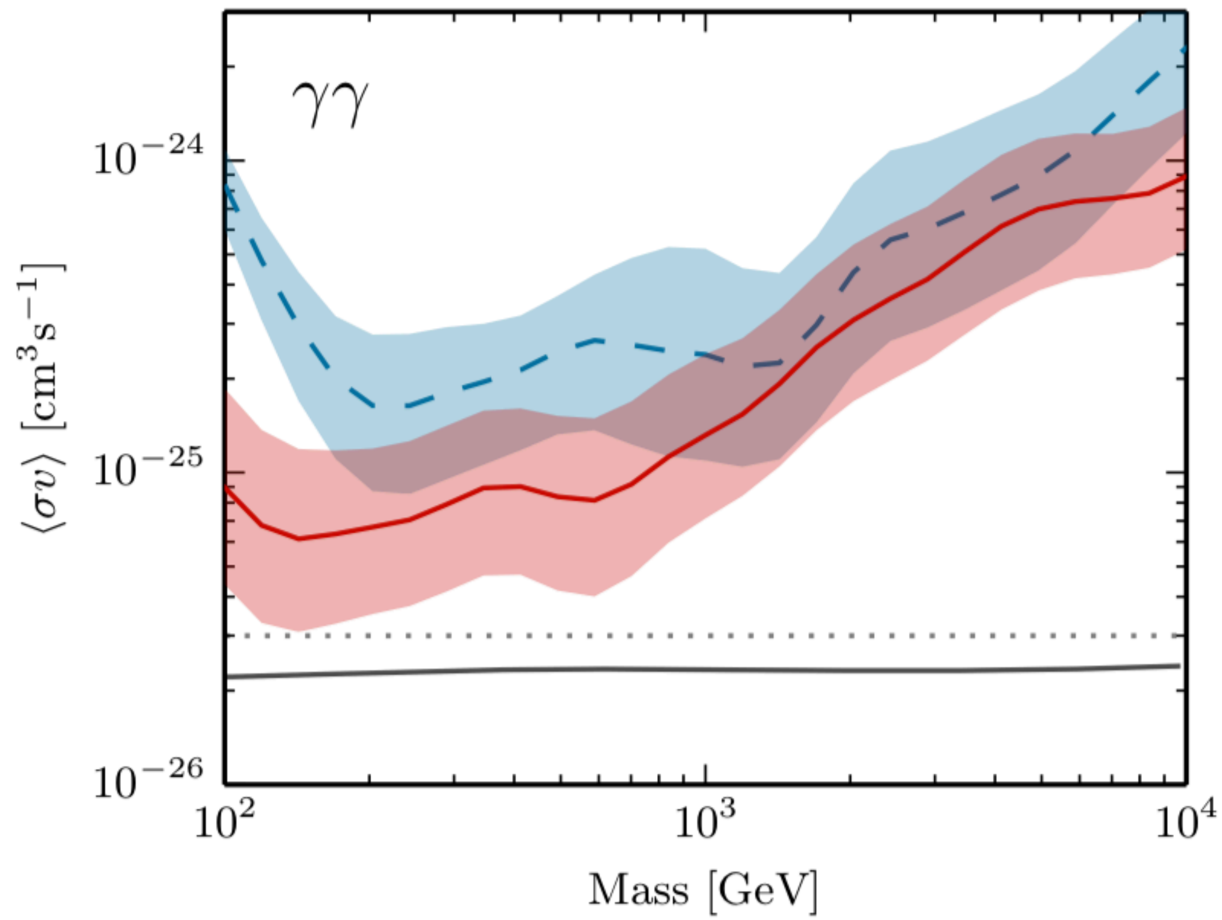

Combined analysis of dSphs from 2007 to 2013

Annihilation cross section limits from the combined dwarves analysis

T. Junk, Nucl. Instrum. Methods Phys. Res., Sect. A 434, 435 (1999)

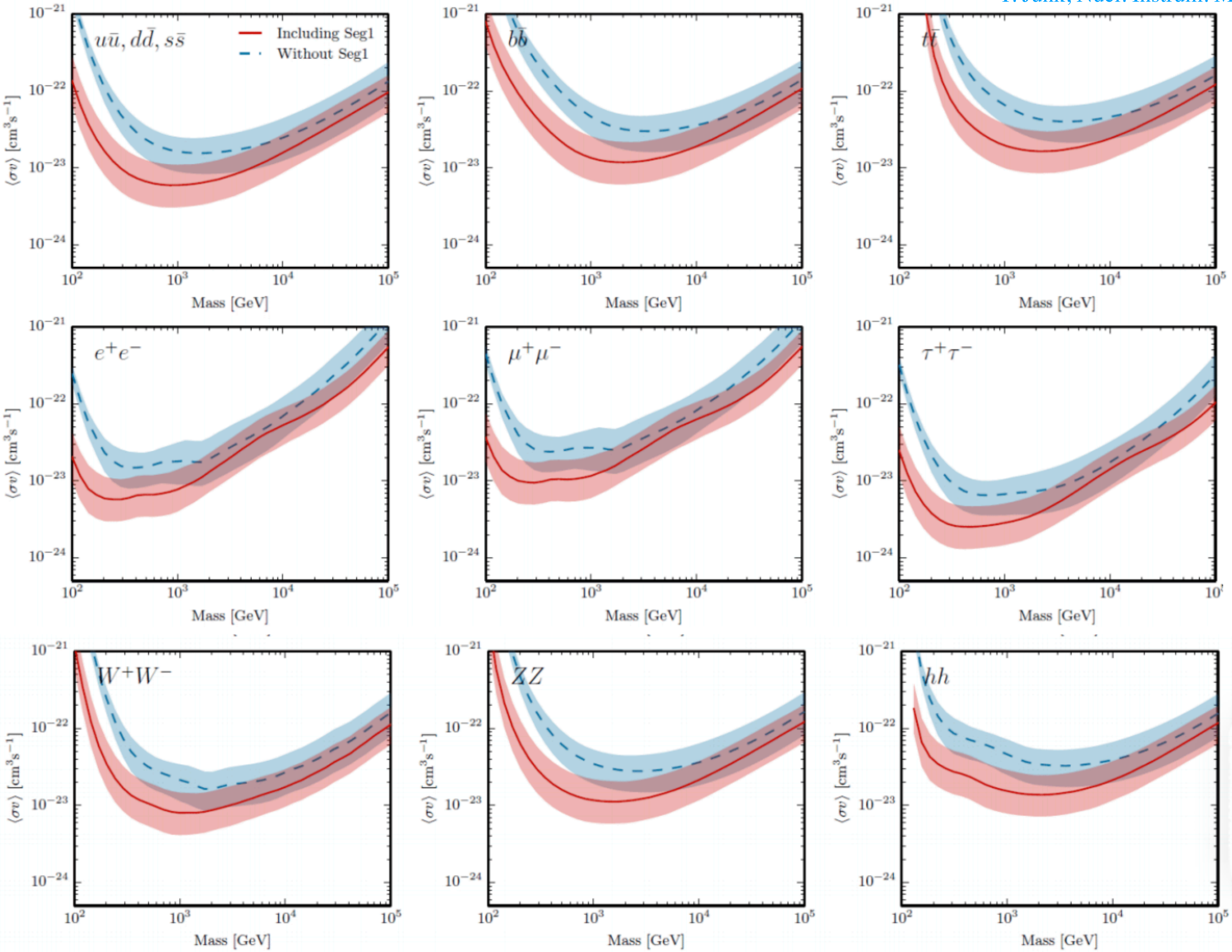

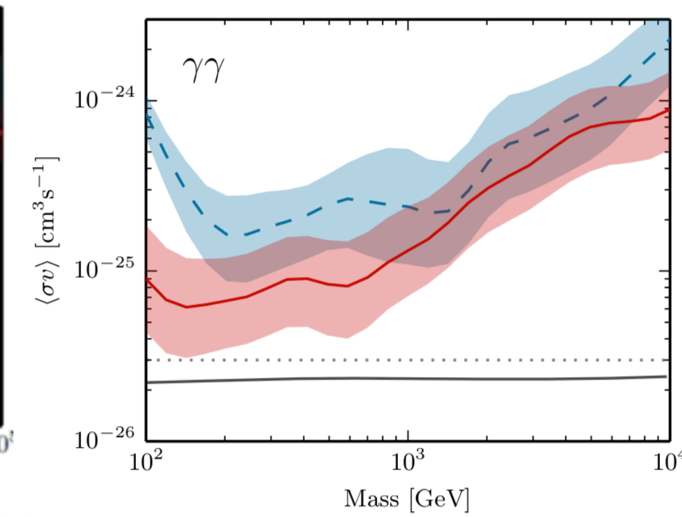

Two orders of magnitude away from relic abundance

$$\langle \sigma v \rangle \simeq 2.2 \times 10^{-26}\ \mathrm{cm}^3$$

Combined analysis of dSphs from 2007 to 2013

Expected annihilation cross section limits from the combined dwarves analysis

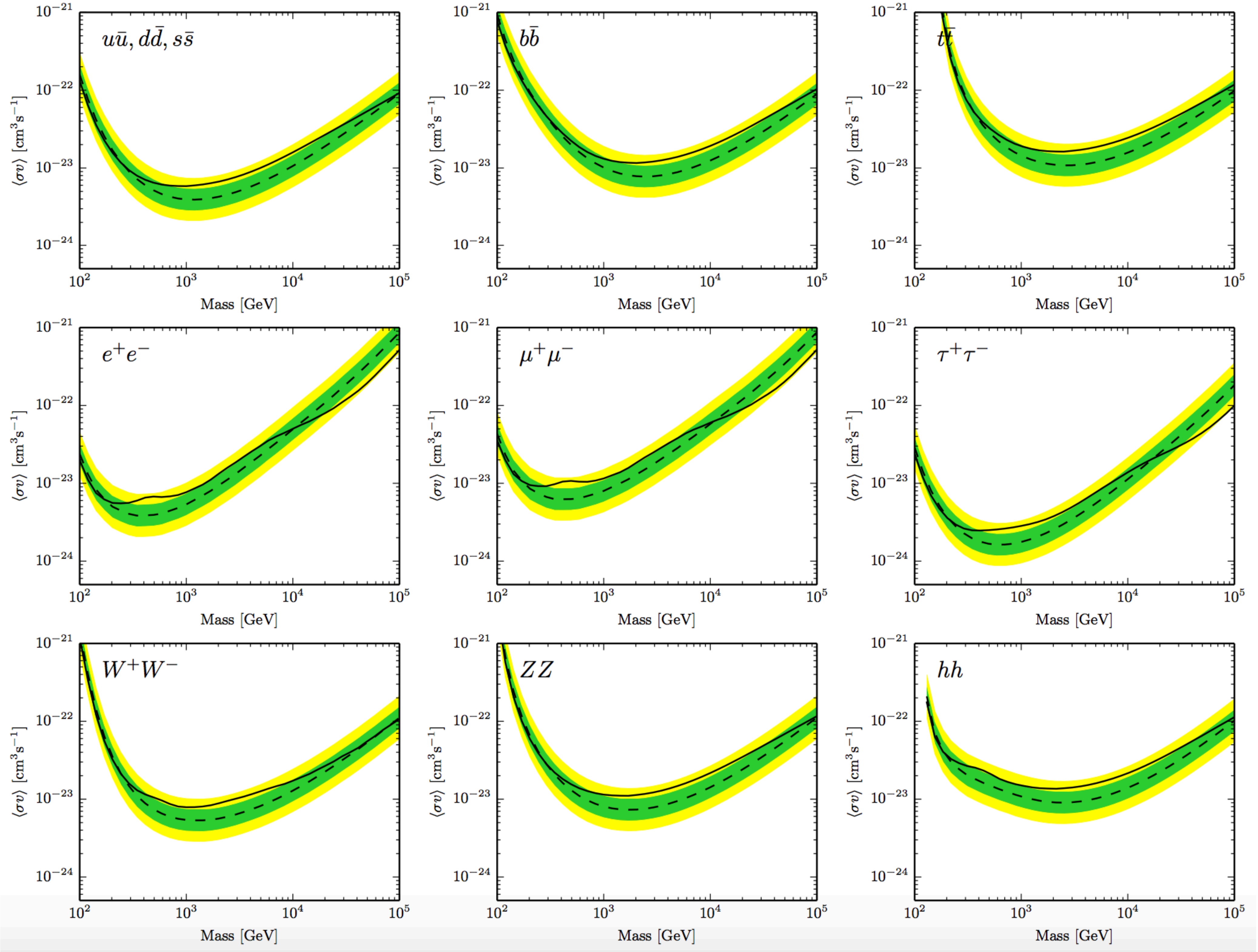

Combined analysis of dSphs from 2007 to 2013

Comparison with other experiments

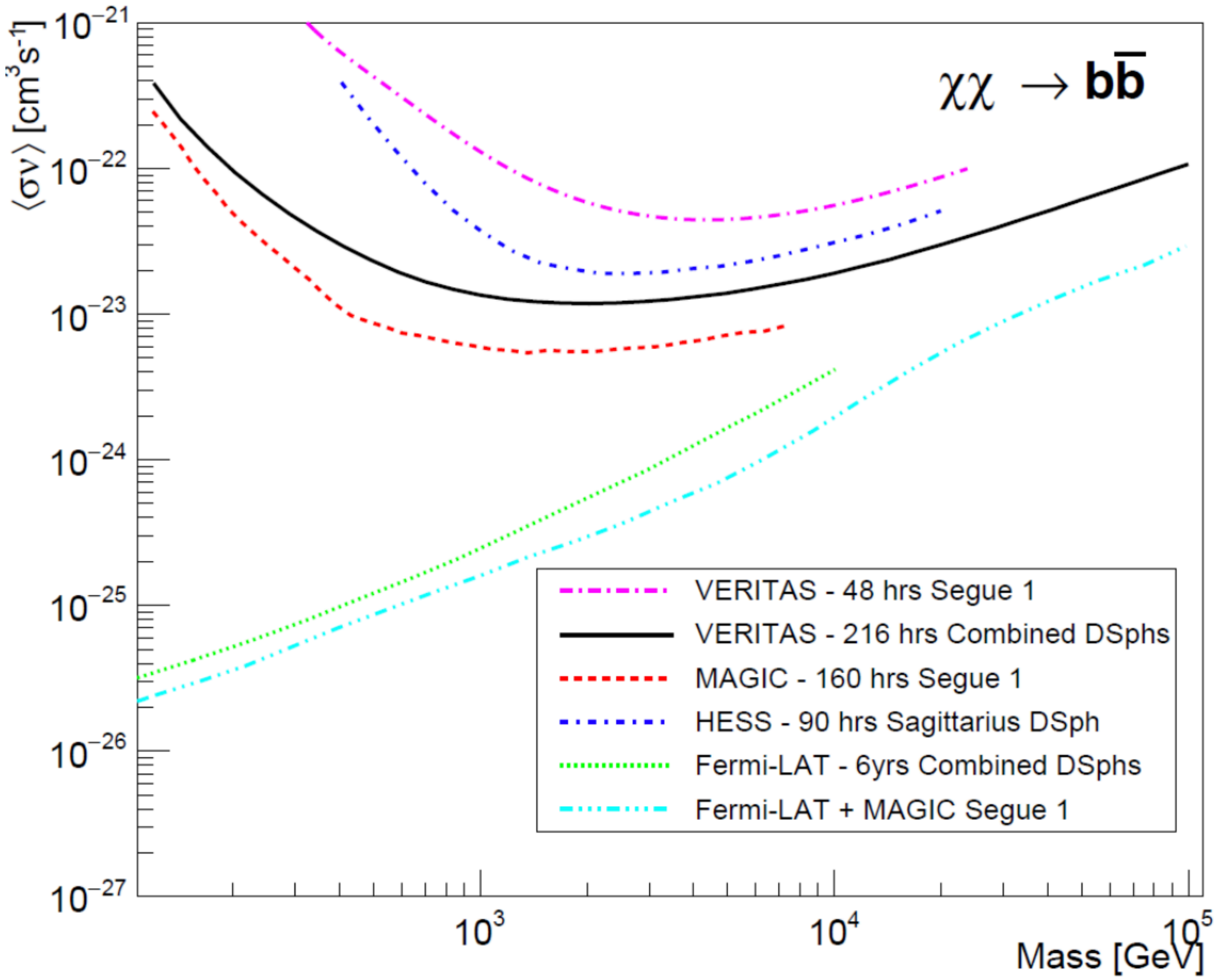

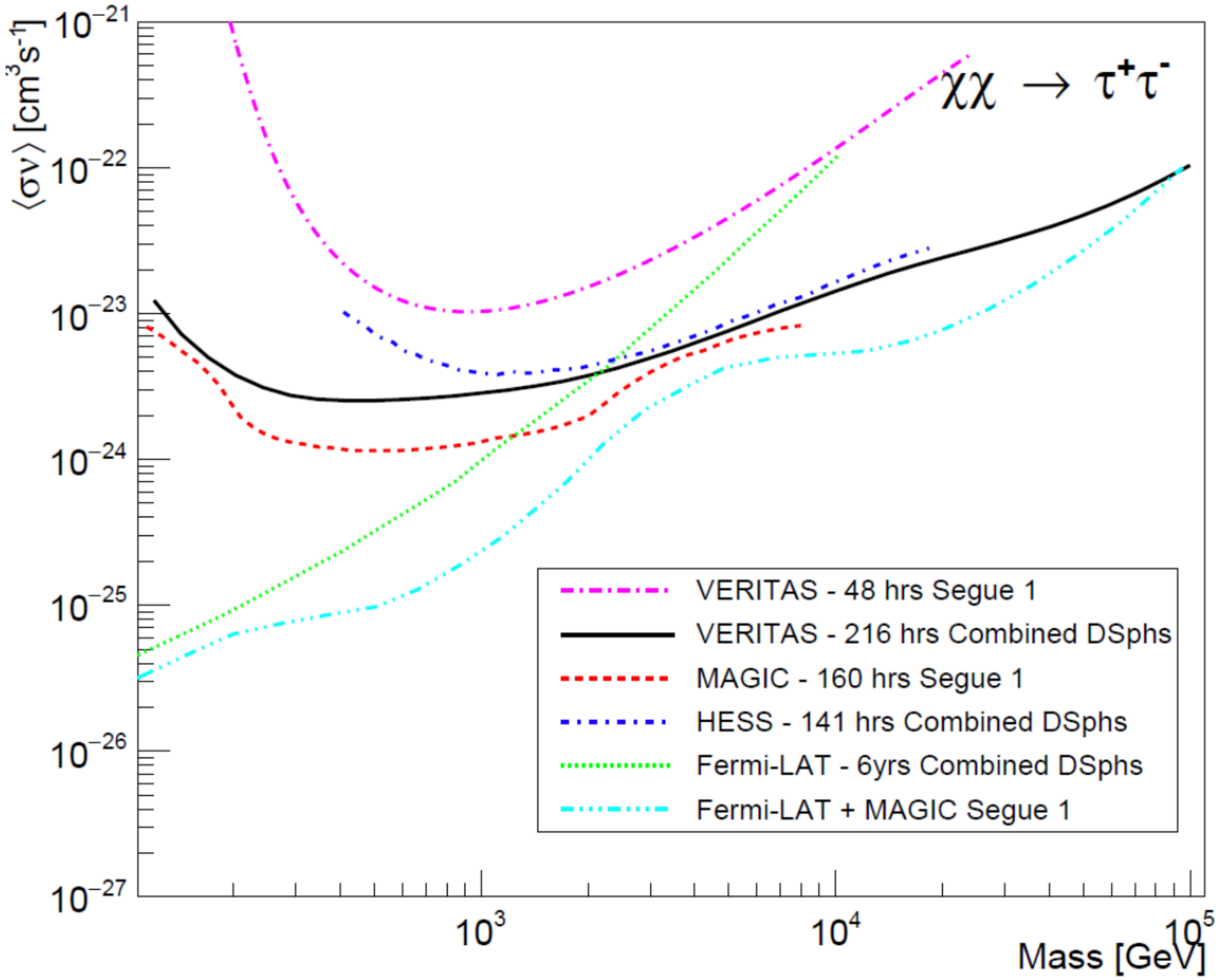

- Improvement respect to 48 hrs on Segue 1

VERITAS dSphs observations: Ursa Major II

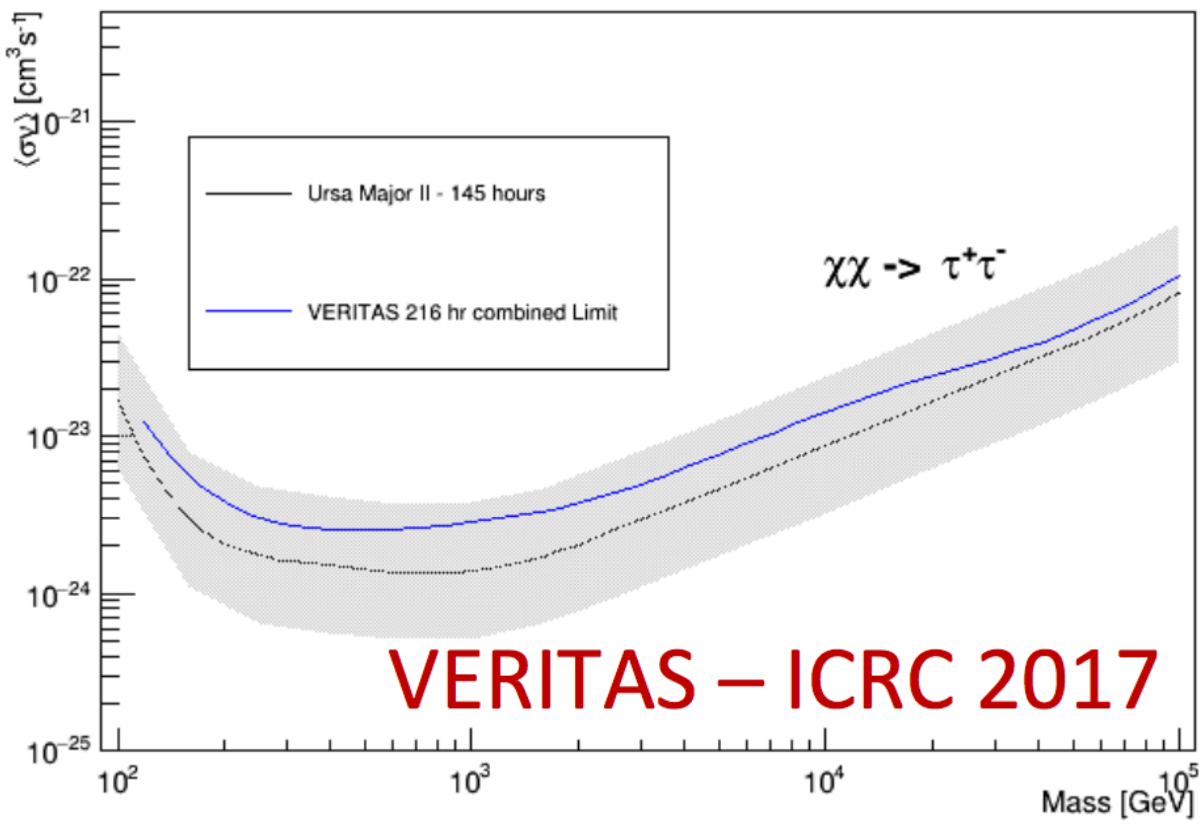

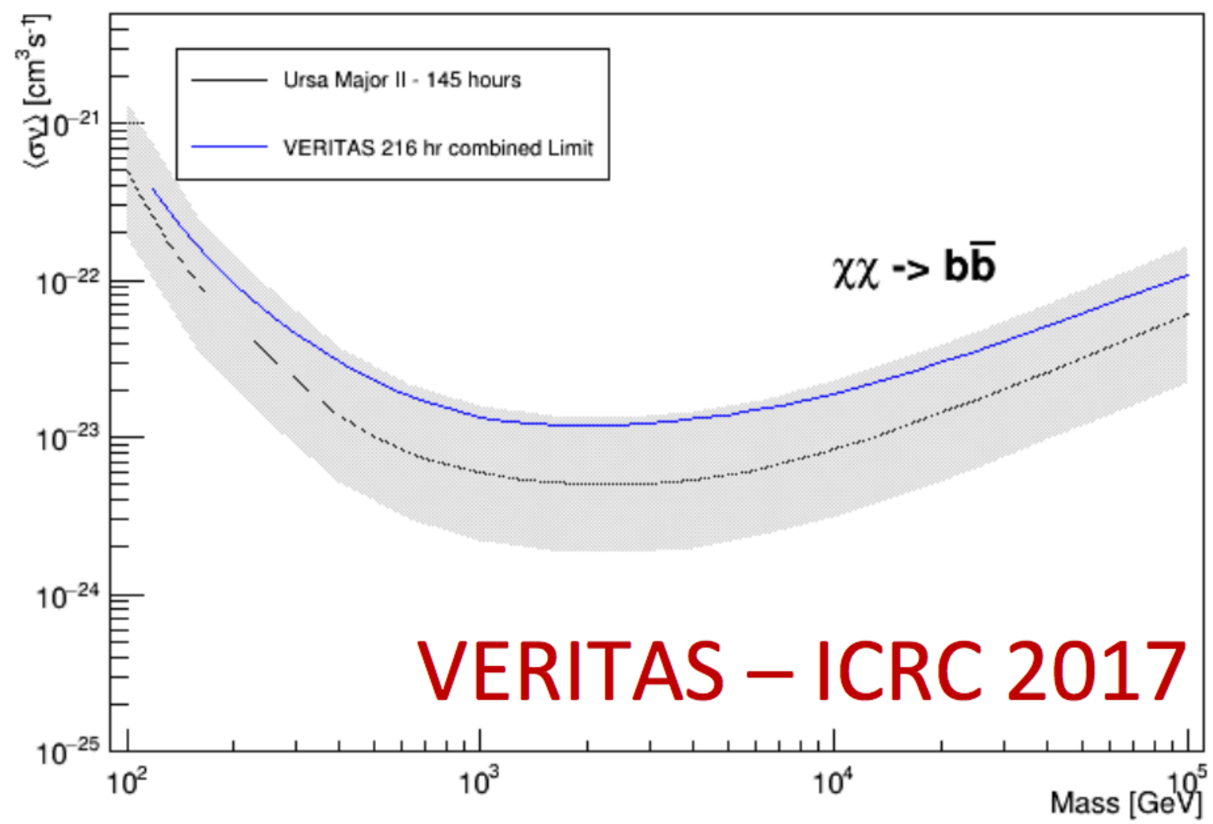

- Observed with VERITAS from 2013-2017
- **145 hrs** after quality cuts
- **An excess of 1σ found** at Ursa Major II position
- **Flux upper limit** $1.4 \times 10^{-8} m^{-2} s^{-1}$ above 200 GeV at a 95% c.l.
- Unbinned Maximum Likelihood used to compute limits (Aleksić et al., 2014)
- Annihilation spectrum from PPPC 4 DM ID (Cirelli et al., 2011)
- Ursa Major II limit is **more constraining** up to 30% than combined limit

Future work

VERITAS has huge dSphs dataset still to be analysed

- Extended analysis for dSphs
- Analysis with *Boosted decision trees for gamma-hadron separation*
- Analysis with image template method
  (Christiansen, J. & the VERITAS Collaboration)

Future work

VERITAS has huge dSphs dataset still to be analysed

- Extended analysis for dSphs
- Analysis with *Boosted decision trees for gamma-hadron separation*
- Analysis with image template method
  (Christiansen, J. & the VERITAS Collaboration)

Improved sensitivity to weak DM signal

Conclusions and perspectives

1. VERITAS published **combined results** using 216 hrs in the energy range 100 GeV-100TeV
2. VERITAS put **integral flux upper limit above 300 GeV** for each dSph
3. VERITAS has a larger dataset: **new data from 2013-2018** still to be analysed
4. **More sensitive analysis techniques**: *Boosted decision trees* and image template method to **improve the sensitivity** and look for weaker sources
5. Analysis of dSphs as (slightly) **extended sources**
6. **Joint binned likelihood analysis** with MAGIC, H.E.S.S., Fermi-LAT and HAWC (extends up to higher and lower energies) → **GloryDuck Project**

THANKS FOR YOUR ATTENTION

Back-up slides

Conclusions and perspectives

GloryDuck Project

Source name	Observed by	Number of observed hours / Exposure
Boötes 1	VERITAS	14.0
Carina	H.E.S.S.	22.9
Coma Berenices	H.E.S.S.	10.9
Draco	VERITAS	49.8
Fornax	H.E.S.S.	6.0
Ursa Major II	MAGIC	94.8
Ursa Minor	VERITAS	60.4
Sagittarius	H.E.S.S.	85.5
Sculptor	H.E.S.S.	11.8
Segue 1	MAGIC	43.2
	VERITAS	92.0
Willman 1	VERITAS	13.6

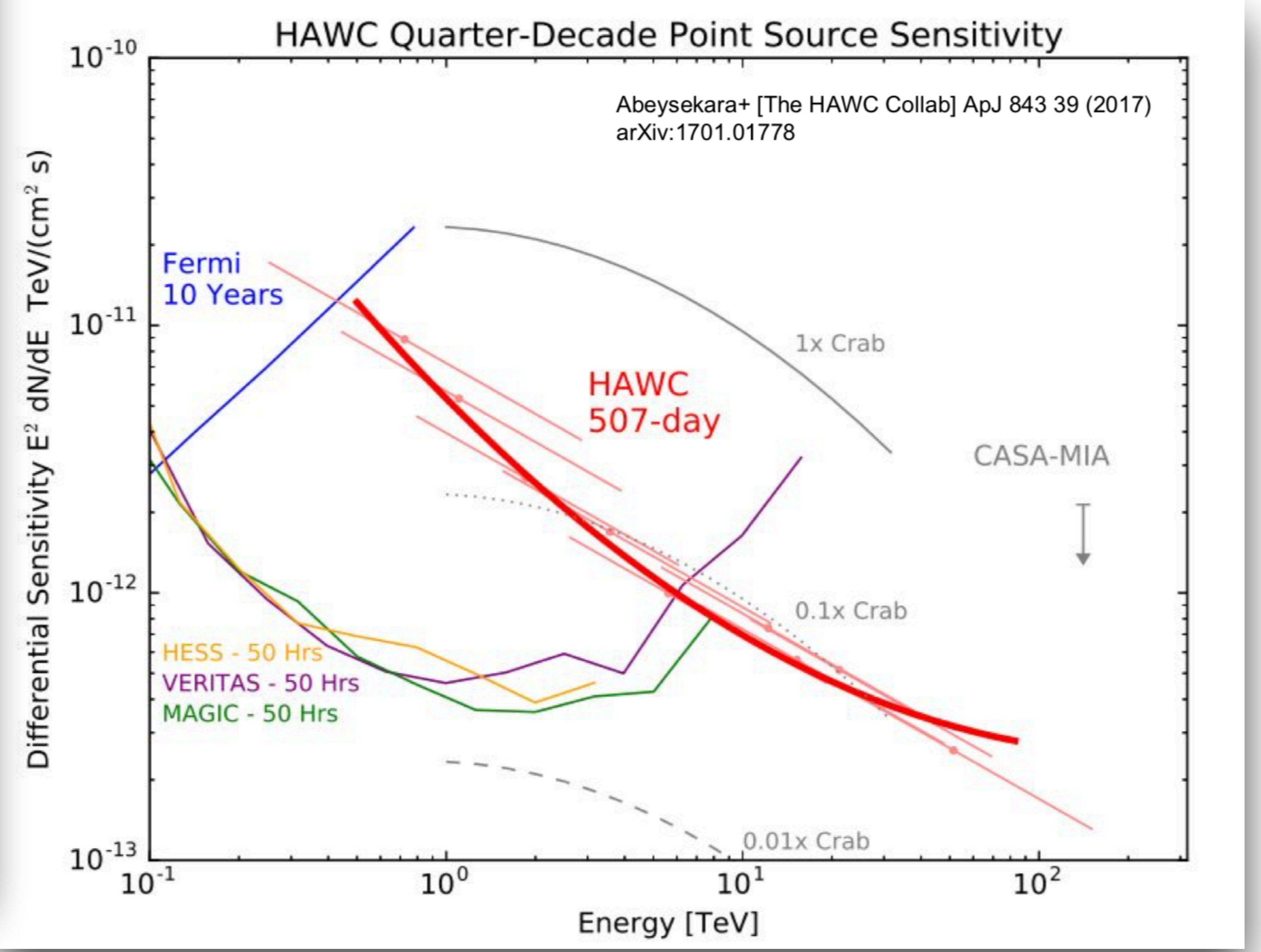

Flux upper limits

DSph	N_{ON} [counts]	N_{OFF} [counts]	$\bar{\alpha}$	Significance [σ]	$N^{95\%}$ [counts]	$\Phi^{95\%}$ [10^{-12} cm^{2}s^{-1}]	Distance [kpc]	$\log_{10} J(0.17°)$ [GeV^2 cm^{-5}]
Segue 1	15895	120826	0.131	0.7	235.8	0.34	23	$19.2^{+0.3}_{-0.3}$
Draco	4297	39472	0.111	-1.0	33.5	0.15	76	$18.3^{+0.1}_{-0.1}$
Ursa Minor	4181	35790	0.119	-0.1	91.6	0.37	76	$18.9^{+0.3}_{-0.3}$
Boötes 1	1206	10836	0.116	-1.0	34.5	0.40	66	$18.3^{+0.3}_{-0.4}$
Willman 1	1926	18187	0.108	-0.6	23.5	0.39	38	N/A

Bounded profile likelihood ratio statistical method from Rolke et al., 2005

$$\Phi_\gamma(> E_{\rm min}) = N_{\gamma,\rm obs}(> E_{\rm min}) \int_{E_{\rm min}}^{\infty} \frac{dN_\gamma}{dE}\, dE \times \left[\sum_j \int_{E_{\rm min}}^{\infty} \tau_j A_{{\rm eff},j}(E) \frac{dN_\gamma}{dE}\, dE \right]^{-1}$$

Estimation of r_{max}

Given a star

$$P(z|R) \propto \left(1+\frac{z^2+R^2}{R_e^2}\right)^{-5/2}$$

Probability of its line-of-sight distance z proportional to Plummer profile

$$P(r|R) = \int P(r|z,R)\,P(z|R)\,dz$$

Probability distribution for the unprojected distance r, given the projected distance R

If r>R $$\mathrm{CDF}(r|R) = \int_0^r P(r'|R)\,dr' = \frac{(r^2-R^2)^{1/2}\,(r^2+\frac{1}{2}(3R_h^2+R^2))}{(r^2+R_h^2)^{3/2}}$$

$$\mathrm{CDF}_{\max}(r|R_1,\ldots,R_n) = \mathrm{CDF}(r|R_1)\cdots\mathrm{CDF}(r|R_n)$$